



GRB 211227A as a Peculiar Long Gamma-Ray Burst from a Compact Star Merger

Hou-Jun Lü¹ , Hao-Yu Yuan¹, Ting-Feng Yi² , Xiang-Gao Wang¹, You-Dong Hu³, Yong Yuan⁴, Jared Rice⁵, Jian-Guo Wang⁶, Jia-Xin Cao¹, De-Feng Kong¹, Emilio Fernandez-García³, Alberto J. Castro-Tirado^{3,7}, Ji-Shun Lian¹, Wen-Pei Gan¹, Shan-Qin Wang¹ , Li-Ping Xin⁸, M. D. Caballero-García³, Yu-Feng Fan⁶, and En-Wei Liang¹

¹ Guangxi Key Laboratory for Relativistic Astrophysics, School of Physical Science and Technology, Guangxi University, Nanning 530004, People's Republic of China; lhj@gxu.edu.cn, lew@gxu.edu.cn

² Key Laboratory of Colleges and Universities in Yunnan Province for High-energy Astrophysics, Department of Physics, Yunnan Normal University, Kunming 650500, People's Republic of China

³ Instituto de Astrofísica de Andalucía (IAA-CSIC), Glorieta de la Astronomía s/n, E-18008, Granada, Spain

⁴ School of Physics Science And Technology, Wuhan University No.299 Bayi Road, Wuhan, Hubei, People's Republic of China

⁵ Department of Physics, Texas State University, San Marcos, TX 78666, USA

⁶ Yunnan Observatories, Chinese Academy of Sciences, Kunming, People's Republic of China

⁷ Unidad Asociada al CSIC Departamento de Ingeniería de Sistemas y Automática, Escuela de 16 Ingeniería Industrial, Universidad de Málaga, Málaga, Spain

⁸ CAS Key Laboratory of Space Astronomy and Technology, National Astronomical Observatories, Chinese Academy of Sciences, Beijing 100101, People's Republic of China

Received 2022 January 21; revised 2022 May 7; accepted 2022 May 10; published 2022 May 30

Abstract

Long-duration gamma-ray bursts (GRBs) associated with supernovae (SNe) are believed to originate from massive star core-collapse events, whereas short-duration GRBs that are related to compact star mergers are expected to be accompanied by kilonovae. GRB 211227A, which lasted about 84 s, had an initial short/hard spike followed by a series of soft gamma-ray extended emission at redshift $z = 0.228$. We performed follow-up observations of the optical emission using BOOTES, LCOGT, and the Lijiang 2.4 m telescope, but we detected no associated supernova signature, even down to very stringent limits at such a low redshift. We observed the host galaxy within a large error circle and roughly estimated the physical offset of GRB 211227A as 20.47 ± 14.47 kpc from the galaxy center. These properties are similar to those of GRB 060614, and suggest that the progenitor of GRB 211227A is not favored to be associated with the death of massive stars. Hence, we propose that GRB 211227A originates from a compact star merger. Calculating pseudo-kilonova emission for this case by adopting the typical parameters, we find that any associated pseudo-kilonova is too faint to be detected. If this is the case, it explains naturally the characteristics of the prompt emission, the lack of SN and kilonova emission, and the large physical offset from the galaxy center.

Unified Astronomy Thesaurus concepts: [Gamma-ray bursts \(629\)](#)

1. Introduction

Gamma-ray bursts (GRBs) are thought to originate in violent events, such as a massive star core-collapse or compact star mergers (Paczynski 1986; Woosley 1993; also see Kumar & Zhang 2015 for a review). Such catastrophic destruction of these progenitor systems may result in the formation of a magnetar or black hole, which powers a relativistic jet pointing in the direction of the observer (e.g., Eichler et al. 1989; Usov 1992; Thompson 1994; Dai & Lu 1998a, 1998b; Popham et al. 1999; Zhang & Mészáros 2001; Narayan et al. 2001; Lei et al. 2009; Metzger et al. 2011; Bucciantini et al. 2012; Berger 2014; Lü & Zhang 2014). Within the standard fireball model scenario, the observed variability of γ -ray emission is caused by photosphere emission (Thompson 1994; Ghisellini & Celotti 1999; Pe'er et al. 2006; Lazzati & Begelman 2010; Beloborodov 2010), internal shocks (Rees & Meszaros 1994; Sari & Piran 1997), or internal collision-induced magnetic reconnection and turbulence (ICMART; Zhang & Yan 2011). A multiwavelength afterglow emission is attributed to the external shock when the fireball is decelerated by a sufficient

amount of external material (Mészáros & Rees 1997; Sari et al. 1998).

Phenomenally, GRBs are divided as long- and short-duration with a division line at the observed duration $T_{90} \sim 2$ s (Kouveliotou et al. 1993). From a theoretical point of view, long-duration GRBs are powered by a relativistic jet that breaks out of the envelope of a massive star when it undergoes core-collapse. There is about $0.1 M_{\odot}$ of nickel that can also be created via explosive nucleosynthesis during this collapse. Therefore, a bright optical/infrared transient called a supernova (SN; Woosley & Bloom 2006; Hjorth & Bloom 2012) should be produced when the ^{56}Ni decays into cobalt. Naturally, some long-duration GRBs are associated with an SN when the distance is not large enough (Galama et al. 1998; Kippen et al. 1998; Hjorth et al. 2003; Stanek et al. 2003; Malesani et al. 2004; Della Valle et al. 2006; Mazzali et al. 2008; Bufano et al. 2012; Xu et al. 2013; Cano et al. 2017; Lü et al. 2018). On the other hand, the short-duration GRBs are believed to have originated from compact star mergers. The leading candidates are neutron star–neutron star (NS–NS) and neutron star–black hole (NS–BH) systems. The NS–NS merger may result in a magnetar as a remnant (Rosswog et al. 2000; Dai et al. 2006; Metzger et al. 2010; Yu et al. 2013; Zhang 2013; Lasky et al. 2014; Lü et al. 2015) or black hole (Rosswog et al. 2014). If this is the case, a mildly isotropic, subrelativistic ejecta with 10^{-4} – $10^{-2} M_{\odot}$ and 0.1 – $0.3c$, can be ejected during

the merger to heat ejecta (Hotokezaka et al. 2013; Rosswog et al. 2014). So that, an optical/infrared transient that is powered by radioactive decay from r -process radioactive materials may be detected from any direction if the flux is high enough (Li & Paczyński 1998; Kulkarni 2005; Metzger et al. 2010; Barnes & Kasen 2013), and the transient is known as a macronova, kilonova, or mergernova (Kulkarni 2005; Metzger et al. 2010; Yu et al. 2013).

Observationally, the first GRB–SN association event was discovered as the underluminous GRB 980425 and the Type Ic SN 1998bw at redshift $z = 0.0085$ (Galama et al. 1998; Kippen et al. 1998; Pian et al. 1998; Sadler et al. 1998). Afterwards, a handful of long-duration GRBs associated with spectroscopically identified Type Ib/c SNe were detected (Kovacevic et al. 2014; Cano et al. 2016; Lü et al. 2018). By comparing with the first GRB–SN association, the first kilonova emission event from a compact star merger was discovered in GRB 130603B with an excess near-IR emission matching the predictions for r -process emission (Fan et al. 2013; Berger et al. 2013; Tanvir et al. 2013; Fong et al. 2014). After that, several short GRBs were claimed to be associated with a kilonova or mergernova, e.g., GRB 050709 (Jin et al. 2016), GRB 060614 (Yang et al. 2015), GRB 070809 (Jin et al. 2020), GRB 080503 (Gao et al. 2015), GRB 160821B (Kasliwal et al. 2017; Lamb et al. 2019; Troja et al. 2019), and GRB 150101B (Troja et al. 2018). Gao et al. (2017) carried out a complete search for magnetar-powered mergernovae from a sample of Swift GRBs, and found that three magnetar-powered mergernova candidates are associated with short GRBs (050724, 061006, and 070714B) from late optical observations. Rastinejad et al. (2021) presented a comprehensive optical and near-infrared catalog to search for possible kilonova emission and to constrain its ejecta mass (also see Yuan et al. 2021).

A particularly interesting case, GRB 060614, which is a nearby long-duration GRB at $z = 0.125$ (Della Valle et al. 2006; Fynbo et al. 2006; Gal-Yam et al. 2006; Gehrels et al. 2006), needs to be mentioned again. The light curve of GRB 060614 is characterized by a short/hard spike (with a duration ~ 5 s) followed by a series of soft gamma-ray extended emission⁹ with a duration ~ 100 s. Phenomenologically, it definitely belongs to the long-duration GRB population and a bright SN was expected. It should have been detected at such a low redshift, but an SN association was not detected even with a deep search. These facts are consistent with the compact star merger scenario, but they are not the direct evidence (Gehrels et al. 2006; Zhang et al. 2007a). There was an ongoing debate on the physical origin of this case until 2015. Possible evidence of a kilonova from SN-less long-duration GRB 060614 was claimed (Yang et al. 2015). They discovered a near-infrared bump (only two data points) that is significantly above the regular decaying afterglow, and therefore claimed it to be a signature of the kilonova component.

GRB 211227A is potentially associated with a galaxy at redshift $z = 0.228$ (Beardmore et al. 2021; Malesani et al. 2021). The light curve of its prompt emission is very similar to that of GRB 060614, which also has no SN association at this low redshift. However, the difference with GRB 060614 is that we do not find any kilonova signature with GRB 211227A.

One question is what is the progenitor of GRB 211227A: massive star collapse or compact star merger? In this paper, we systematically analyze the observational data of both prompt emission and afterglow, and the host galaxy (in Section 2). Then, comparisons to GRB 211227A and GRB 060614 are shown in Section 3. In Section 4, we attempt to investigate the possible origin by calculating the SN and kilonova emissions. The conclusions are drawn in Section 5 with some additional discussion. Throughout the paper, a concordance cosmology with parameters $H_0 = 71 \text{ km s}^{-1} \text{ Mpc}^{-1}$, $\Omega_M = 0.30$, and $\Omega_\Lambda = 0.70$ is adopted.

2. The Observations and Data Analysis

2.1. Swift BAT Observations

GRB 211227A triggered the Burst Alert Telescope (BAT) at 23:32:06 UT on 2021 December 27 (Beardmore et al. 2021). We downloaded the BAT data from the Swift website¹⁰, and used the standard HEASOFT tools (version 6.28) to process the BAT data. For more details on the analysis, please refer to Sakamoto et al. (2008), Zhang et al. (2009), and Lü et al. (2020). We extract the light curves in different energy bands with a 128 ms time bin (Figure 1). The light curve shows a complex structure with a total duration of about $T_{90} = 84$ s, an initial short/hard spike (with a duration ~ 4 s) followed by a series of soft gamma-ray extended emission with a duration ~ 80 s.

We also extract the spectrum by invoking Xspec for fitting, and the background is extracted by choosing two time intervals with 80 s before and after the burst. Due to the narrow energy band of Swift/BAT, the time-integrated spectrum of the GRB 211227A prompt emission is well fitted by a simple power-law model ($N \propto E^{-\Gamma}$) with an index $\Gamma = 1.53 \pm 0.03$. Moreover, we also separate the light curve into two time slices: the initial hard spike (0.1–4 s) and the long-lasting extended emission (4–84 s). The spectra of both time slices can be fitted by a power-law model with $\Gamma_1 = 1.67 \pm 0.08$ and $\Gamma_2 = 1.5 \pm 0.03$, respectively (see Figure 2). The bottom panel of Figure 1 shows a strong temporal evolution of the spectrum, with $\Gamma \sim 1.5$ at the beginning and $\Gamma \sim 2$ near the end. The fluence in the 15–150 keV band is $8.2 \pm 0.2 \times 10^{-6} \text{ erg cm}^{-2}$, which corresponds to isotropic energy $E_{\text{iso}} \sim 1.14 \times 10^{51} \text{ ergs}$ by adopting $z = 0.228$ in this energy band.

2.2. Swift X-Ray Telescope Observations

The Swift X-ray telescope (XRT) began observing the field at 73.5 s after the BAT trigger. We made use of the public data from the Swift archive¹¹ (Perri et al. 2021). The X-ray light curve in the early time seems to be a broken power-law decay with indices $\alpha_1 = 0.2 \pm 0.08$, $\alpha_2 = 3.10 \pm 0.31$, and break time $t_b = 103 \pm 12$ s (see Figure 4). We also extract the time-resolved spectra of the initial X-ray tail with a power-law model, and the spectrum shows a strong temporal evolution that tracked hard to soft. The time-integrated spectrum of the GRB 211227A in X-ray emission is fitted by a simple power-law model with an index $\Gamma = 1.11 \pm 0.07$, and the column density of hydrogen N_H is $(2.2 \pm 0.5) \times 10^{21} \text{ cm}^{-2}$.

⁹ The observed extended emission is softer than that of the initial short/hard spike of short GRBs and gamma-ray emission of typical long GRBs. The extended emission detected in the BAT band seems to be simply the internal plateau emission when the emission is bright and hard enough (Lü et al. 2015).

¹⁰ <https://www.swift.ac.uk/archive/selectseq.php?tid=01091101&source=obs>

¹¹ https://www.swift.ac.uk/xrt_curves/01091101

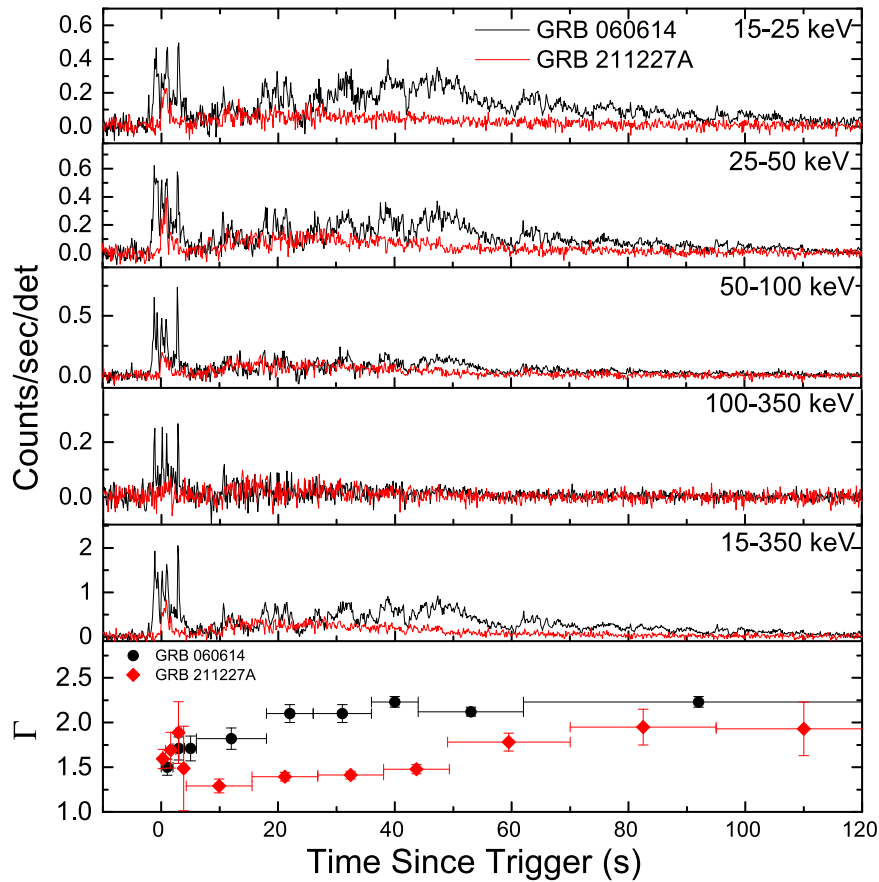


Figure 1. Swift/BAT light curves of GRB 211227A in different energy bands with a 128 ms time bin (red solid lines) and the spectral evolution (red diamonds). In order to compare with GRB 060614, we also plot the light curve (black solid lines) and spectral evolution (black points) in the same panels.

2.3. BOOTES Follow-up Observations

The Burst Observer and Optical Transient Exploring System (BOOTES) followed GRB 211227A with two 60 cm robotic telescopes at BOOTES-2/TELMA station in La Mayora (Malaga, Spain) and BOOTES-4/MET station at the Lijiang Astronomical Observatory (Yunnan, China). The BOOTES-2/TELMA telescope performed two epoch observations at 2021 December 27.99 UT and 2021 December 28.93 UT and the BOOTES-4/MET telescope took four epoch observations at 2021 December 28.69 UT, 2021 December 29.61 UT, 2022 January 03.75 UT, and 2022 January 04.69 UT, respectively. A series of images were obtained using clear and Sloan-*i* filters with exposures of 10 s, 60 s, and 90 s (Hu et al. 2021). The burst’s optical afterglow is not detected in the stacked images of each epoch, which are calibrated via nearby comparison stars from the Sloan Digital Sky Survey (SDSS) catalog for the *i*-filter data or through the transformation equation for the clear filter data. The obtained upper limits within 3σ are listed in Table 1, and the value of extinction (A_V) is 0.062.

2.4. Lijiang 2.4 m Optical Observations

In order to observe the potential optical emission, on 2022 January 3 (~ 6.8 days after trigger), we observed the field of GRB 211227A with the Lijiang 2.4 m telescope, which is located at the Lijiang Observatory of Yunnan Observatories, Chinese Academy of Science (Wang et al. 2019; Xin et al. 2020). The photometric observations were performed using the Johnson *R*-band filter with a total exposure of 1200 s at an

airmass of 1.2 and a seeing of ~ 1.7 under good weather conditions. Three nearby faint stars are in the field of view, which can provide calibration of the target. However, we did not detect any source to a depth of $R > 21.5$ mag within the XRT enhanced error box. On 2022 January 7 (~ 10.7 days after trigger), we observed this field again, with a total exposure time to 1800 s. Again, no signal was detected, and only an upper limit with $R > 21.8$ mag was obtained.

2.5. Other Telescopes’ Follow-up Observations

Besides the BOOTES and Lijiang 2.4 m, there were several ground-optical telescopes that performed follow-up observations of the source after the GRB 211227A trigger, such as the Nanshan/NEXT -0.6 m located at Nanshan, Xinjiang, China (Fu et al. 2021), the LCO 1 m Sinistro instrument at the Teide, Tenerife site (Strausbaugh & Cucchiara 2021), the 2 m robotic Liverpool telescope (Perley 2021), the CAHA 2.2 m telescope at the Calar Alto Observatory, Almeria, Spain (Kann et al. 2021), and the Gemini/GMOS-S (O’Connor et al. 2022). However, none of them could detect any source within upper limits.

2.6. Host Galaxy Observation

We observed the localization of GRB 211227A by using the 1 m telescope at the Las Cumbres Observatory Global Telescope (LCOGT) at the Teide Tenerife site. The observation started at 01:28:37 UT on 2021 December 28 (from 6991 to 8599 s after the BAT trigger), and consisted of 5×300 s

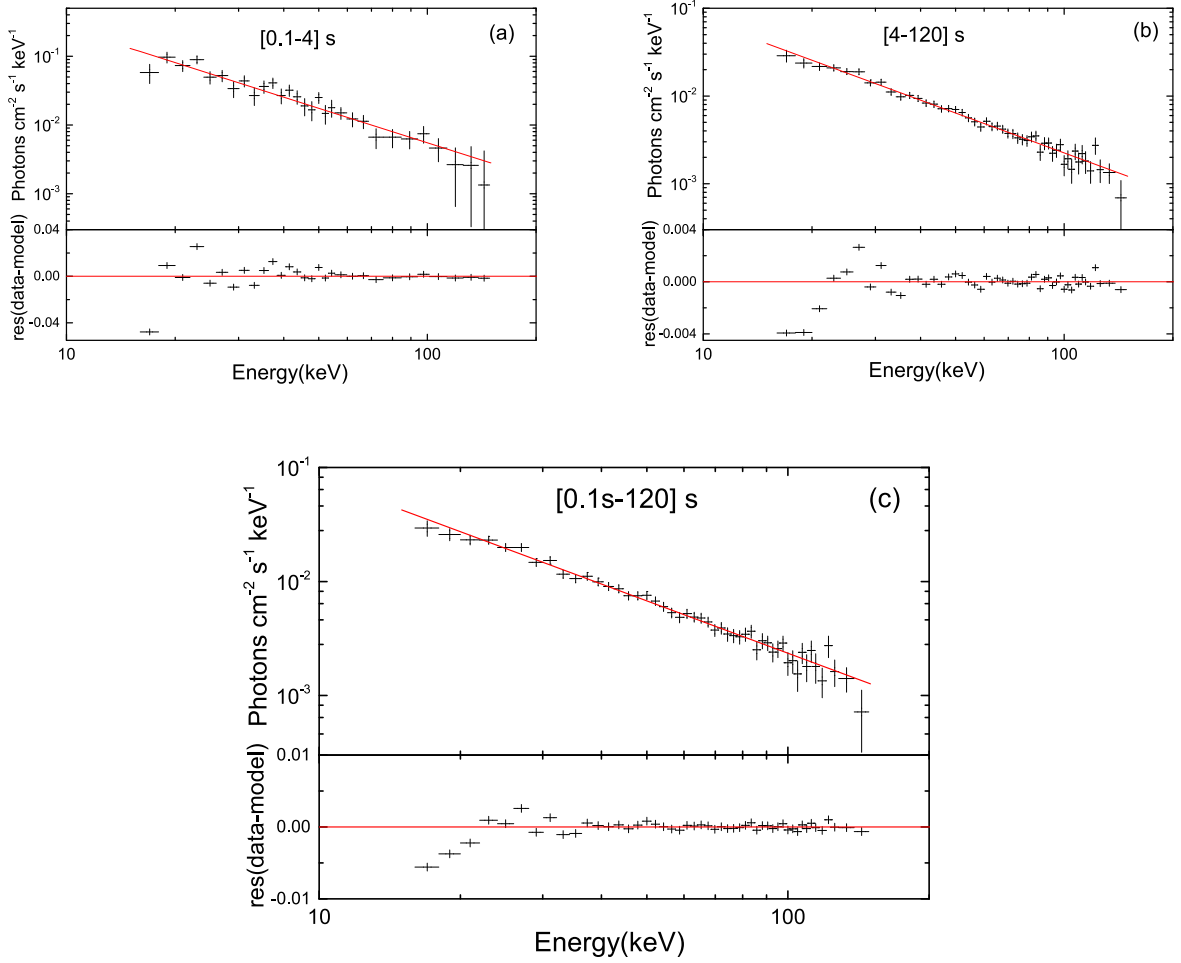


Figure 2. The spectral fits of GRB 211227A with power-law model for time-resolved (a) and (b) and time-integrated (c).

Table 1
Optical Observations of GRB 211227A with BOOTES, LCOGT, and Lijiang 2.4 m in 3σ

T_{start}	T_{end}	$T_{\text{mid}}(s)$	Telescope	Band	Exposure	Magnitude
2021-12-27T23:42:44	2021-12-28T00:01:04	1188	BOOTES-2	clear	40×10	>19.9
2021-12-28T00:36:39	2021-12-28T03:23:28	8877	BOOTES-2	clear	64×60	>20.3
2021-12-28T22:17:41	2021-12-29T00:03:14	85101	BOOTES-2	clear	41×60	>20.1
2021-12-28T16:32:19	2021-12-28T20:18:40	68003	BOOTES-4	clear	92×60	>21.1
2021-12-29T14:43:21	2021-12-29T15:16:54	142081	BOOTES-4	clear	26×60	>20.2
2022-01-03T17:56:17	2022-01-03T20:57:59	590102	BOOTES-4	<i>i</i>	18×90	>20.5
2022-01-04T16:30:15	2022-01-04T17:53:52	668397	BOOTES-4	<i>i</i>	23×90	>21.8
2021-12-28T01:28:37	2021-12-28T01:55:25	7795	LCOGT	<i>R</i>	5×300	>23.81
2022-01-03T18:23:25	2022-01-03T18:43:27	587520	Lijiang-2.4 m	<i>R</i>	1×1200	>21.5
2022-01-07T15:14:28	2022-01-07T15:44:45	924480	Lijiang-2.4 m	<i>R</i>	2×900	>21.8

Note. Not corrected for galaxy extinction.

integrations in the *R* band. Our combined image is centered at 7795 s after the trigger. No afterglow is detected in the XRT error circle in our stacked image down to a limiting magnitude of $R > 23.81$ mag, calculated with respect to the USNO-B.1 catalog. However, there exists a known source at the border of the Swift/XRT error circle at coordinates: R.A. (J2000) = 08:48:35.975 and decl. (J2000) = $-02:44:06.93$, which has $R \sim 19.13 \pm 0.09$ mag from our images, classified as a galaxy with a photoreddshift of $z = 0.244 \pm 0.089$ from SDSS

(Figure 3). Moreover, Malesani et al. (2021) reported that five emission lines are observed in the putative host galaxy (e.g., [O II], Hbeta, [O III], Halpha, [N II], and [S II]), and they proposed that a possible host galaxy of GRB 211227A with redshift $z = 0.228$ was detected by the X-shooter spectrograph. The redshift $z = 0.244 \pm 0.089$ that we measured is consistent with that reported in Malesani et al. (2021) with $z = 0.228$ via the X-shooter spectrograph, and the position of this source for LCOGT observations is the same with the Gamma-ray

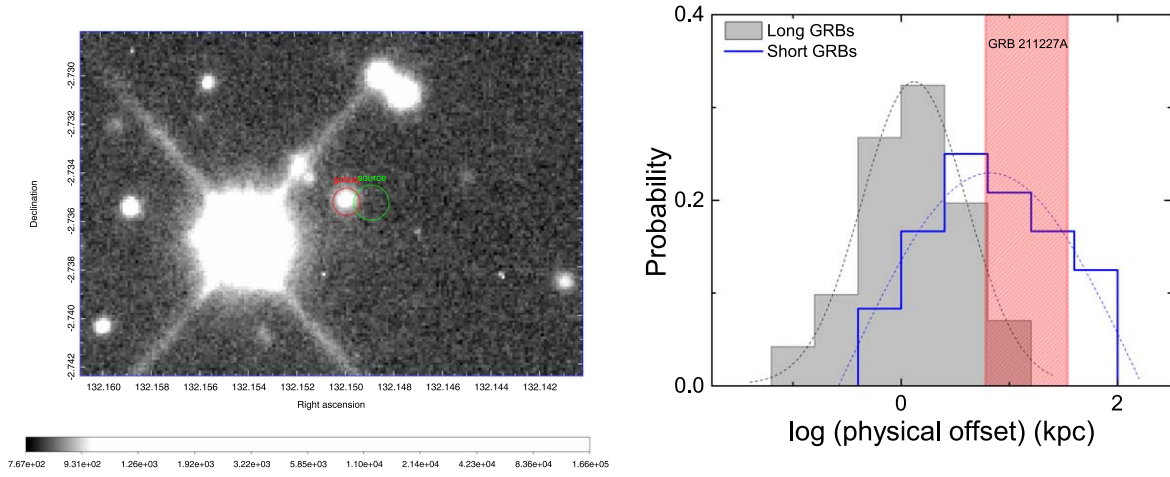


Figure 3. Left: the follow-up observation of GRB 211227A with LCOGT, and the red circle is the location (R.A. = 08:48:35.975, decl. = -02:44:06.93) of the galaxy with a radius of 2'', and the green circle is the location (R.A. = 08:48:35.73, decl. = -02:44:07.1) of the GRB 211227A with an error radius of 2''. Right: distributions of the physical offsets of long and short GRBs taken from Lü et al. (2017), as well as GRB 211227A (vertical solid red line). The dashed lines are the best Gaussian fits for long and short GRBs, respectively.

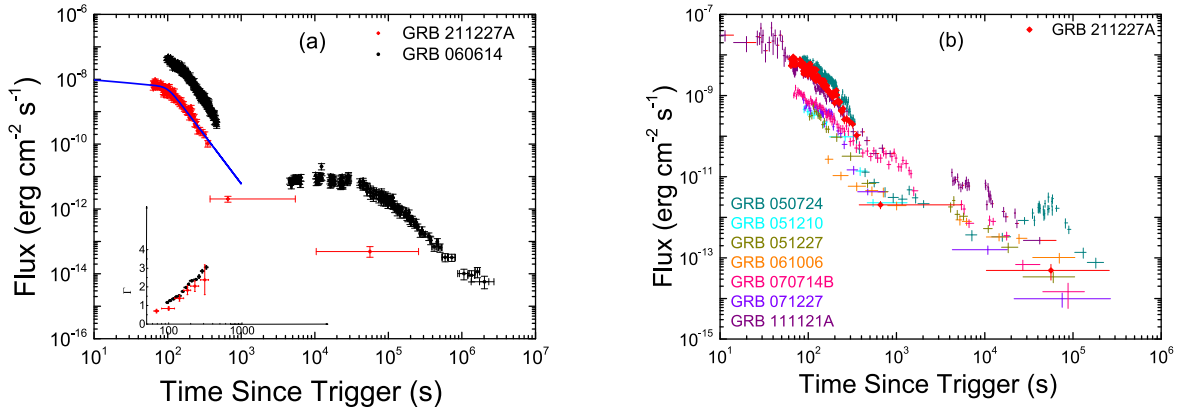


Figure 4. X-ray light curve of GRB 211227A (red diamonds). (a) Comparison with GRB 060614 (blue points), broken power-law model fits (black solid line), and the spectral evolution (insert). (b) Comparison with other short GRBs with extended emission and X-ray plateau observed by Swift from Lü et al. 2015.

Coordinates Network (GCN) report in Malesani et al. (2021). In our calculations, we adopt $z = 0.228$, which is the spectroscopic redshift. In addition, we also calculate the physical distance from the center of GRB 211227A to the host galaxy center as 20.47 ± 14.47 kpc if we assume that the galaxy of $z = 0.228$ is the intrinsic host of GRB 211227A.

3. Comparison with GRB 060614 and Other Short GRBs

From an observational point of view, the duration of GRB 211227A is much longer than that of short-duration GRBs, but is consistent with that of typical long-duration GRBs. Even only considering its initial hard spike lasting ~ 4 s, this burst is still characterized as a category of long-duration GRBs. However, based on the characteristics of the GRB 211227A prompt emission, it is very similar to that of GRB 060614, which had an initial short/hard spike with ~ 5 s followed by a series of soft gamma-ray extended emission lasting ~ 102 s (Gal-Yam et al. 2006; Zhang et al. 2007a). Figure 1 shows the complete comparison of the prompt emission light curves in different energy bands. The profile of the light curves of GRB 211227A and GRB 060614 are consistent with each other, and both of them are characterized by a short/hard spike followed by a series of soft gamma-ray extended emission with a duration ~ 100 s. Moreover, we also present their spectral

evolution, and find that a strong temporal evolution is obvious in both. The evolution behavior of the spectrum is from $\Gamma \sim 1.5$ at the beginning to $\Gamma \sim 2$ near the end. Moreover, the isotropic energy of GRB 211227A is $E_{\text{iso}} \sim 1.14 \times 10^{51}$ ergs, which is also close to that of GRB 060614 with $E_{\text{iso}} \sim 7.76 \times 10^{50}$ ergs.

In terms of the X-ray afterglow, the X-ray emission of GRB 211227A is not a significant difference with other long-duration GRBs that presented several segments (Zhang et al. 2006). The spectrum shows a strong temporal evolution that tracked hard to soft, which is consistent with the behavior of X-ray tail emission in most long- and short-duration GRBs (Zhang et al. 2007b). Figure 4 shows the X-ray emission of GRB 211227A in comparison to that of GRB 060614 (left) and other short GRBs with extended emission (right). We find that the temporal decay index of the X-ray tail before 10^3 s is consistent with that of GRB 060614 ($f \propto t^{-3}$; Zhang et al. 2007b), and shows a similar temporal evolution that tracked from hard to soft. Moreover, we also collect all of the X-ray light curves of the short GRBs with extended emission and plateau emission in X-ray observed by Swift (Lü et al. 2015)¹², and compare with the X-ray emission of GRB 211227A. We

¹² There are seven short GRBs with both extended emission and X-ray plateau emission (e.g., GRBs 050724, 051210, 051227, 061006, 070714B, 071227, and 11121A), and the fraction is about 6% of total short GRBs.

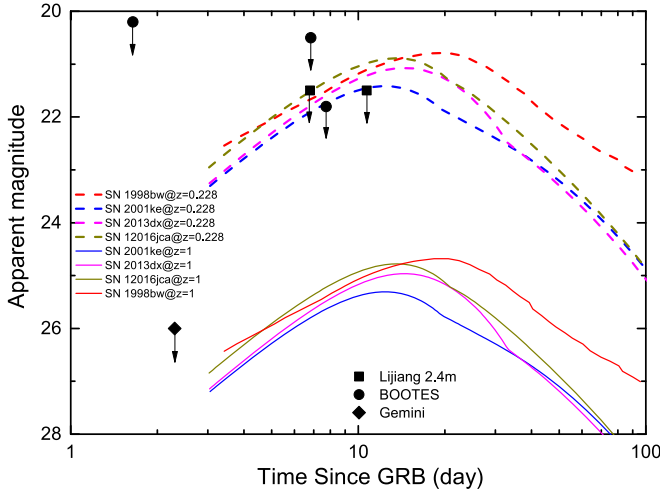


Figure 5. Comparison of the observed data of the GRB 211227A from the Lijiang 2.4 m and BOOTES with those of SN 1998bw, SN 2001ke, SN 2013dx, and SN 2016jca associated with GRBs at $z = 0.228$ (dashed lines) and $z = 1$ (solid lines).

find that the behavior of the early X-ray emission of GRB 211227A is also similar to that of other short GRBs with extended emission.

Moreover, Figure 3 shows the comparison of the physical offset of GRB 211227A with that of other long and short GRBs. We find that the physical offset is larger than that of most long-duration GRBs, but is consistent with the distribution of other short GRBs within a larger error range.

4. Physical Origin: Massive Star Core-collapse or Compact Star Merger?

In general, long-duration GRBs are believed to originate from the deaths of massive stars, and their host galaxies are typically irregular galaxies with intense star formation (Woosley 1993; Fruchter et al. 2006). In contrast, short-duration GRBs are associated with nearby early-type galaxies with little star formation and are related to compact star mergers with a large offset from the center of the host galaxy (Berger et al. 2005; Fong et al. 2010). Moreover, from a statistical point of view, Leibler & Berger (2010) found that the two GRB host populations remain distinct based on the stellar mass distribution and population ages of galaxies. However, such a cozy picture was destroyed by nearby long-duration GRB 060614 without an SN association (Della Valle et al. 2006; Fynbo et al. 2006; Gal-Yam et al. 2006; Gehrels et al. 2006) and short-duration GRB 200826A associated with an SN (Zhang et al. 2021; Ahumada et al. 2021). Interestingly, GRB 211227A shares some similar properties with GRB 060614, and has a large physical offset from the galaxy center. One question is what is the physical origin of GRB 211227A? In this section, we attempt to find some clues to reveal the physical origin of this case.

4.1. Massive Star Core-collapse Scenario

The “smoking gun” signature of a long-duration GRB from a massive star core-collapse is the detection of the associated SN in the optical band (Galama et al. 1998; Kippen et al. 1998; Hjorth et al. 2003; Stanek et al. 2003; Malesani et al. 2004; Della Valle et al. 2006; Mazzali et al. 2008; Bufano et al. 2012; Xu et al. 2013; Cano et al. 2017; Lü et al. 2018). Being a

long-duration GRB 211227A at a low redshift $z = 0.228$, it is expected that an SN component should be detected around 10 days after the trigger, yet it is surprising that deep searches of an underlying SN give null results. This raises interesting questions regarding whether the distance is too large for detecting a less energetic event. Therefore, we shift several SNe to the redshift $z = 0.228$ to see how bright they are. Figure 5 shows light curves of SN 1998bw, SN 2001ke, SN 2013dx, and SN 2016jca associated with some long-duration GRBs at $z = 0.228$. We find that the upper limit of the luminosity of the SN (also the limiting magnitude of the Lijiang 2.4 m telescope with the limit luminosity as $(4.3\text{--}5.6) \times 10^{42} \text{ erg s}^{-1}$), if any, is several times fainter than SN 1998bw and fainter than other Type Ic SNe associated with GRBs at $z = 0.228$ (Galama et al. 1998; Della Valle et al. 2003; Xu et al. 2013; Cano et al. 2017). It suggests that the lack of an SN associated with GRB 211227A is not caused by too large of a distance, but more likely physical reasons. In order to compare those SNe at $z = 0.228$ with that of a higher redshift, we replot those SNe if we put them into $z = 1$. It is much dimmer than the upper limits of observations. On the other hand, based on the upper limit of observations, one can roughly estimate the redshift $z = 0.285$ of SNe that can be ruled out. Moreover, the measurement of a large physical offset is also inconsistent with that of other long GRBs. From the prompt emission analysis, on the other hand, GRB 211227A is consistent with the properties of GRB 060614. Those facts suggest that it does not likely match with the physical properties expected in a massive star core-collapse. If so, the lack of an SN signature is a natural expectation. However, the origin of the massive star collapse of GRB 211227A is still to be ruled out if it occurs in the host galaxy with a higher redshift.

4.2. Compact Star Mergers Scenario

The direct detection of GW170817 and its electromagnetic counterpart (e.g., GRB 170817A and AT2017gfo), which was the first identified multimessenger gravitational-wave and electromagnetic signal, originated in the merger of a binary NS system (Abbott et al. 2017; Covino et al. 2017; Goldstein et al. 2017; Savchenko et al. 2017; Zhang et al. 2018). The observations of kilonova AT2017gfo were comprehensive, long lasting, and multiwavelength, compared to previous kilonova candidates (Valenti et al. 2017; Coulter et al. 2017; Arcavi et al. 2017; Lipunov et al. 2017; Tanvir et al. 2017; Ai et al. 2018; Metzger 2019; Rossi et al. 2020). A rough constraint of kilonova parameters can be realized via a multiwavelength fit with the kilonova model (Yu et al. 2018; Ai et al. 2018; Li et al. 2018). By adopting the same parameters ($M_{\text{ejc}} \sim 0.03 M_{\odot}$, $\beta \sim 0.25c$, and $\kappa \sim 0.97 \text{ cm}^2 \text{ g}^{-1}$) with kilonova AT2017gfo, one can also calculate the kilonova emission of GRB 211227A in K , R , and U bands at redshift $z = 0.228$ (see Figure 7). The peak magnitude is not much of an improvement, and it remains fainter than the observed limitation.

Yang et al. (2015) reported the discovery of a near-infrared bump that is inconsistent with the afterglow emission of GRB 060614, but arises from a kilonova. They invoke the kilonova model to fit the excess in the near-infrared band with the ejecta mass ($M_{\text{ejc}} \sim 0.1 M_{\odot}$), velocity ($\beta \sim 0.2c$), and opacity ($\kappa \sim 10 \text{ cm}^2 \text{ g}^{-1}$). In order to compare the kilonova emission between GRB 211227A and GRB 060614, we calculate the possible kilonova emission by adopting the same parameters

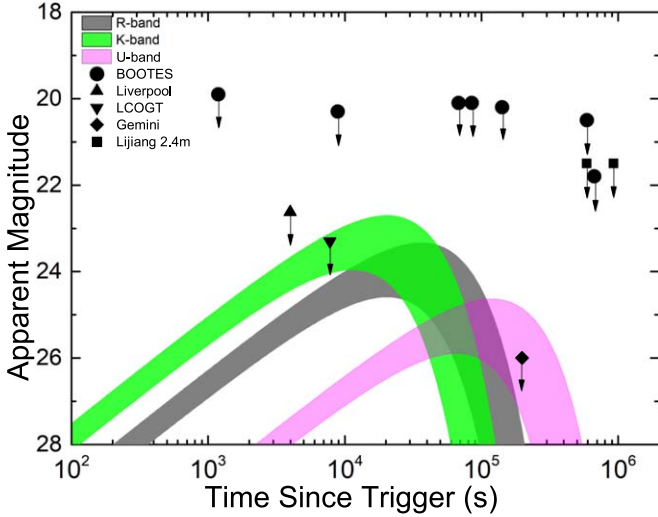


Figure 6. Light curve of kilonova in K , R , and U bands of GRB 211227A by adopting $M_{\text{ejc}} \sim (0.01 - 0.1) M_{\odot}$, $\beta \sim 0.2c$, and $\kappa \sim 10 \text{ cm}^2 \text{ g}^{-1}$ at $z = 0.228$.

with that of GRB 060614 even with the large uncertainty. Figure 6 shows the kilonova emission in K , R , and U bands at redshift $z = 0.228$ by considering only one energy source. Here, the ejecta mass range $(0.01 - 0.1) M_{\odot}$ is adopted in our calculations. The peak magnitude of kilonova emission is much lower than the observed limitation of the Lijiang 2.4 m and current other optical telescopes. If so, the lack of a kilonova signature is the natural expectation for a less energetic event.

Inspired by GRB 170817A and GRB 060614, we propose that the long-duration GRB 211227A is from a more energetic merger event. Moreover, the large physical offset (~ 20.47 kpc) of this case that is larger than that of most long GRBs, is also supported by this hypothesis, and is even still consistent with several long GRBs within a large error. In general, robust associations of a fainter-than-supernova optical/IR transient (called kilonova) with some GRBs suggest that they are likely related to NS–NS or NS–BH mergers (Tanvir et al. 2013; Abbott et al. 2017; Yang et al. 2015; Goldstein et al. 2017; Savchenko et al. 2017; Troja et al. 2017; Zhang et al. 2018). Such a transient is powered by the r -process (rapid neutron capture) and radioactive decay of the synthesized heavy elements (e.g., Li & Paczyński 1998; Freiburghaus et al. 1999; Arcavi et al. 2017; Coulter et al. 2017; Valenti et al. 2017; Lipunov et al. 2017; Tanvir et al. 2017). If GRB 211227A is from a compact star merger, one can roughly calculate how bright it is by adopting some typical parameters.

For an NS–NS merger, additional energy should be injected into the ejecta if the postmerger remnant is an NS (Metzger et al. 2010; Yu et al. 2013; Ai et al. 2018; Yu et al. 2018; Yuan et al. 2021). We also invoke a model of hybrid energy sources (r -process and energy injection from the NS) to calculate the kilonova emission. Lü et al. (2015) proposed that both extended emission and an internal plateau can be produced by magnetar spin-down.¹³ The observed extended emission (EE) and X-ray tail of GRB 211227A seems to come from the contribution of a magnetar spin-down. If this is the case, we adopt the same parameters as above in the r -process, and $L_0 = 10^{48} \text{ erg s}^{-1}$ and $t = 105 \text{ s}$ as the initial luminosity and

¹³ In other words, the extended emission is essentially the brightest internal plateau commonly observed in short GRBs, and a more sensitive and softer detector would detect more EE from short GRBs

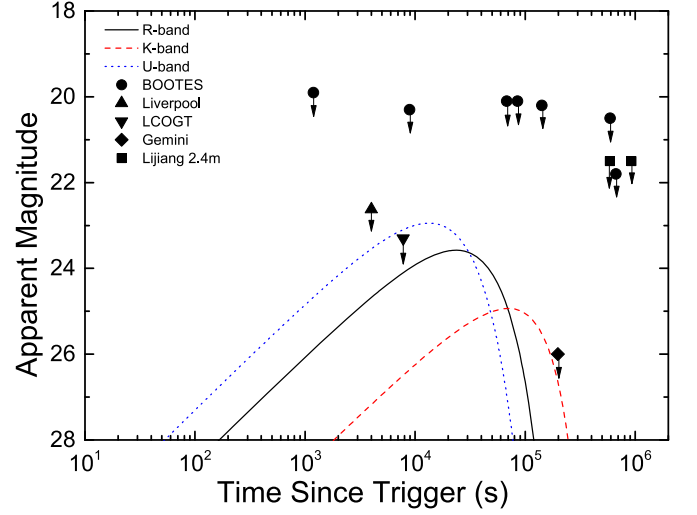


Figure 7. Calculated kilonova emission of GRB 211227A at $z = 0.228$ by considering one energy source with $M_{\text{ejc}} \sim 0.03 M_{\odot}$, $\beta \sim 0.25c$, and $\kappa \sim 0.97 \text{ cm}^2 \text{ g}^{-1}$, which are taken from kilonova AT2017gfo (Yu et al. 2018).

timescale of energy injection from an NS. We find that the peak magnitude is also not improved even when considering hybrid energy sources, because the timescale of energy injection is too short to be contributed to the kilonova. Hence, the progenitor of GRB 211227A seems to come from compact star mergers, which can naturally explain the lack of SN and kilonova emission, the characteristic of prompt emission, the initial X-ray emission, and the large physical offset.

5. Conclusion and Discussion

GRB 211227A was observed by Swift to have a duration of $\sim 84 \text{ s}$ at redshift $z = 0.228$, but the light curve is characterized by an initial short/hard spike (with a duration $\sim 4 \text{ s}$) followed by a series of soft gamma-ray extended emission with a duration $\sim 80 \text{ s}$. Both the prompt emission and the X-ray initial tail of this case show a strong temporal evolution that tracked from hard to soft, and those behaviors are very similar to that of GRB 060614. Several optical telescopes made follow-up observations of the afterglow and host galaxy, but did not detect any afterglow emission except for upper limitations. We also applied for the Lijiang 2.4 m optical telescope to observe this event twice, but obtained only upper limits. Based on the LCOGT observations, we can roughly estimate the physical offset from the galaxy center as $20.47 \pm 14.47 \text{ kpc}$.

At such a low redshift, it is expected that an SN component should be detected around 10 days after the trigger if we believe the massive star core-collapse origin, yet it is surprising that deep searches of an underlying SN give null results. We shift several SN events that are associated with long-duration GRBs into the redshift $z = 0.228$, and find that the upper limit of the luminosity of the SN, if any, is several times fainter than SN 1998bw, and fainter than other Type Ic SNe associated with GRBs at $z = 0.228$. The lack of an associated SN and the large physical offset of this case suggests that the progenitors of GRB 211227A do not seem to originate from a massive star core-collapse. If so, the lack of an SN signature and the large physical offset are a natural expectation.

Alternatively, we propose that the long-duration GRB 211227A is from a compact star merger. If this is the case, we also calculate the kilonova emission by adopting the same

parameters with that of GRB 060614 and GRB 170817A, and find that the kilonova emission is too faint to be detected. Hence, the progenitor of GRB 211227A seems to come from compact star mergers, which can naturally interpret the lack of SN and kilonova emissions, the characteristics of the prompt emission, and the large physical offset. Moreover, Kann et al. (2011) used a large sample of GRB afterglow data to compare the optical afterglows of Type I (originated from a compact star merger) and Type II GRBs (related to the death of massive star), and found that the optical afterglow of Type I GRBs are intrinsically lower than that of Type II GRBs. The lack of optical afterglow of GRB 211227A also supports its origin in a compact star merger.



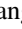

On the other hand, GRB 211227A is a possible optically dark burst. Melandri et al. (2012) studied the properties of the population of completely optically dark GRBs that were observed by Swift, and presented the relationship between optical flux and X-ray flux that was observed at $t = 11$ hr for a complete sample of optically dark GRBs. In order to test this possibility, we also calculate the upper limits of both optical and X-ray flux observed at $t = 11$ hr, and find that both the observed optical and X-ray flux at $t = 11$ hr are much lower than that of optically dark bursts identified in Melandri et al. (2012). So, the possibility that GRB 211227A is an optically dark GRB cannot be ruled out. If this is the case, GRB 211227A should be generated in much denser environments in the host galaxy. Moreover, another possibility is that the GRB 211227A is not the host at $z = 0.228$, but located at a higher redshift with a faint and underlying galaxy that we do not observe by the deepest upper limit of the field. Bloom et al. (2002) and Lyman et al. (2017) pointed out that one can calculate the probability of chance coincidence of a possible host galaxy. Following the method of those two papers, we also roughly estimate the probability of chance coincidence $P_{\text{ch}} = 0.038$, which is less than 0.1 ($P_{\text{ch}} \geq 0.1$ for no obvious host (Bloom et al. 2002)). So, the galaxy at $z = 0.228$ seems to be the host of GRB 211227A.

In order to investigate the progenitor of a GRB 211227A-like event, more information on the host galaxy is essential. We therefore encourage intense multiband, more sensitive optical follow-up observations of GRB 211227A-like events to catch electromagnetic signals (e.g., kilonova or SN signatures) and the properties of the host galaxy in the future. If possible, the observed GRB 211227A-like event with a gravitational-wave signal will also provide a good probe to study progenitors.

We are very grateful to thank the referee for constructive comments and suggestions to improve this manuscript. We also thank WeiKang Zheng and Meng-Hua Chen for helpful comments. We acknowledge the use of the public data from the Swift data archive. This work is supported by the National Natural Science Foundation of China (grant Nos. 11922301, 12133003, and U1938201), the Guangxi Science Foundation (grant Nos. 2017GXNSFFA198008 and AD17129006), the Program of Bagui Young Scholars Program (LHJ), the teaching reform project of Guangxi Higher education (2019JGZ102), and special funding for Guangxi distinguished professors (Bagui Yingcai and Bagui Xuezheng). A.J.C.T. acknowledges support from the Spanish Ministry project PID2020-118491GB-I00 and the collaboration with the rest of IAA-CSIC ARAE group and the UMA Unidad Asociada to CSIC colleagues. M.C.G. acknowledges support from the Ramón y

Cajal Fellowship RYC2019-026465-I. Y.D.H. acknowledges support under the additional funding from RYC2019-026465-I.

ORCID iDs

Hou-Jun Lü  <https://orcid.org/0000-0001-6396-9386>
 Ting-Feng Yi  <https://orcid.org/0000-0001-8920-0073>
 Shan-Qin Wang  <https://orcid.org/0000-0001-7867-9912>
 En-Wei Liang  <https://orcid.org/0000-0002-7044-733X>

References

- Abbott, B. P., Abbott, R., Abbott, T. D., et al. 2017, *PhRvL*, **119**, 161101
 Ahumada, T., Singer, L. P., Anand, S., et al. 2021, *NatAs*, **5**, 917
 Ai, S., Gao, H., Dai, Z.-G., et al. 2018, *ApJ*, **860**, 57
 Arcavi, I., Hosseinzadeh, G., Howell, D. A., et al. 2017, *Natur*, **551**, 64
 Barnes, J., & Kasen, D. 2013, *ApJ*, **775**, 18
 Beardmore, A. P., Barthelmy, S. D., Marshall, F. E., et al. 2021, GCN, 31316
 Beloborodov, A. M. 2010, *MNRAS*, **407**, 1033
 Berger, E. 2014, *ARA&A*, **52**, 43
 Berger, E., Fong, W., & Chornock, R. 2013, *ApJL*, **774**, L23
 Berger, E., Price, P. A., Cenko, S. B., et al. 2005, *Natur*, **438**, 988
 Bloom, J. S., Kulkarni, S. R., & Djorgovski, S. G. 2002, *AJ*, **123**, 1111
 Bucciantini, N., Metzger, B. D., Thompson, T. A., et al. 2012, *MNRAS*, **419**, 1537
 Bufano, F., Pian, E., Sollerman, J., et al. 2012, *ApJ*, **753**, 67
 Cano, Z., Johansson Andreas, K. G., & Maeda, K. 2016, *MNRAS*, **457**, 2761
 Cano, Z., Wang, S.-Q., Dai, Z.-G., & Wu, X.-F. 2017, *AdAst*, **2017**, 8929054
 Coulter, D. A., Foley, R. J., Kilpatrick, C. D., et al. 2017, *Sci*, **358**, 1556
 Covino, S., Wiersema, K., Fan, Y. Z., et al. 2017, *NatAs*, **1**, 791
 Dai, Z. G., & Lu, T. 1998a, *MNRAS*, **298**, 87
 Dai, Z. G., & Lu, T. 1998b, *A&A*, **333**, L87
 Dai, Z. G., Wang, X. Y., Wu, X. F., et al. 2006, *Sci*, **311**, 1127
 Della Valle, M., Chincarini, G., Panagia, N., et al. 2006, *Natur*, **444**, 1050
 Della Valle, M., Malesani, D., Benetti, S., et al. 2003, *A&A*, **406**, L33
 Eichler, D., Livio, M., Piran, T., et al. 1989, *Natur*, **340**, 126
 Fan, Y.-Z., Yu, Y.-W., Xu, D., et al. 2013, *ApJL*, **779**, L25
 Fong, W., Berger, E., & Fox, D. B. 2010, *ApJ*, **708**, 9
 Fong, W., Berger, E., Metzger, B. D., et al. 2014, *ApJ*, **780**, 118
 Freiburghaus, C., Rosswog, S., & Thielemann, F.-K. 1999, *ApJL*, **525**, L121
 Fruchter, A. S., Levan, A. J., Strolger, L., et al. 2006, *Natur*, **441**, 463
 Fu, S. Y., Zhu, Z. P., Liu, X., et al. 2021, GCN, 31320
 Fynbo, J. P. U., Watson, D., Thöne, C. C., et al. 2006, *Natur*, **444**, 1047
 Gal-Yam, A., Fox, D. B., Price, P. A., et al. 2006, *Natur*, **444**, 1053
 Galama, T. J., Vreeswijk, P. M., van Paradijs, J., et al. 1998, *Natur*, **395**, 670
 Gao, H., Ding, X., Wu, X.-F., et al. 2015, *ApJ*, **807**, 163
 Gao, H., Zhang, B., Lü, H.-J., et al. 2017, *ApJ*, **837**, 50
 Gehrels, N., Norris, J. P., Barthelmy, S. D., et al. 2006, *Natur*, **444**, 1044
 Ghisellini, G., & Celotti, A. 1999, *A&AS*, **138**, 527
 Goldstein, A., Veres, P., Burns, E., et al. 2017, *ApJL*, **848**, L14
 Hjorth, J., & Bloom, J. S. 2012, *The Gamma-Ray Burst - Supernova Connection*, Gamma-Ray Bursts (Cambridge: Cambridge Univ. Press), 169
 Hjorth, J., Sollerman, J., Møller, P., et al. 2003, *Natur*, **423**, 847
 Hotokezaka, K., Kiuchi, K., Kyutoku, K., et al. 2013, *PhRvD*, **87**, 024001
 Hu, Y.-D., Sun, T.-R., Fernandez-Garcia, E., et al. 2021, GCN, 31318
 Jin, Z.-P., Covino, S., Liao, N.-H., et al. 2020, *NatAs*, **4**, 77
 Jin, Z.-P., Hotokezaka, K., Li, X., et al. 2016, *NatCo*, **7**, 12898
 Kann, D. A., de Ugarte Postigo, A., Thoene, C. C., et al. 2021, GCN, 31341
 Kann, D. A., Klose, S., Zhang, B., et al. 2011, *ApJ*, **734**, 96
 Kasliwal, M. M., Korobkin, O., Lau, R. M., et al. 2017, *ApJL*, **843**, L34
 Kippen, R. M., Briggs, M. S., Komers, J. M., et al. 1998, *ApJL*, **506**, L27
 Koveliotou, C., Meegan, C. A., Fishman, G. J., et al. 1993, *ApJL*, **413**, L101
 Kovacevic, M., Izzo, L., Wang, Y., et al. 2014, *A&A*, **569**, A108
 Kulkarni, S. R. 2005, arXiv:astro-ph/0510256
 Kumar, P., & Zhang, B. 2015, *PhR*, **561**, 1
 Lamb, G. P., Tanvir, N. R., Levan, A. J., et al. 2019, *ApJ*, **883**, 48
 Lasky, P. D., Haskell, B., Ravi, V., et al. 2014, *PhRvD*, **89**, 047302
 Lazzati, D., & Begelman, M. C. 2010, *ApJ*, **725**, 1137
 Lei, W. H., Wang, D. X., Zhang, L., et al. 2009, *ApJ*, **700**, 1970
 Leibler, C. N., & Berger, E. 2010, *ApJ*, **725**, 1202
 Li, L.-X., & Paczyński, B. 1998, *ApJL*, **507**, L59
 Li, S.-Z., Liu, L.-D., Yu, Y.-W., et al. 2018, *ApJL*, **861**, L12
 Lipunov, V. M., Gorbvskoy, E., Kornilov, V. G., et al. 2017, *ApJL*, **850**, L1
 Lü, H.-J., & Zhang, B. 2014, *ApJ*, **785**, 74
 Lü, H.-J., Zhang, B., Lei, W.-H., et al. 2015, *ApJ*, **805**, 89

- Lü, H., Wang, X., Lu, R., et al. 2017, *ApJ*, **843**, 114
- Lü, H.-J., Lan, L., Zhang, B., et al. 2018, *ApJ*, **862**, 130
- Lü, H.-J., Yuan, Y., Lan, L., et al. 2020, *ApJL*, **898**, L6
- Lyman, J. D., Levan, A. J., Tanvir, N. R., et al. 2017, *MNRAS*, **467**, 1795
- Malesani, D. B., Izzo, L., Xu, D., et al. 2021, GCN, 31324
- Malesani, D., Tagliaferri, G., Chincarini, G., et al. 2004, *ApJL*, **609**, L5
- Mazzali, P. A., Valenti, S., Della Valle, M., et al. 2008, *Sci*, **321**, 1185
- Melandri, A., Sbarufatti, B., D'Avanzo, P., et al. 2012, *MNRAS*, **421**, 1265
- Mészáros, P., & Rees, M. J. 1997, *ApJ*, **476**, 232
- Metzger, B. D. 2019, *LRR*, **23**, 1
- Metzger, B. D., Giannios, D., Thompson, T. A., et al. 2011, *MNRAS*, **413**, 2031
- Metzger, B. D., Martínez-Pinedo, G., Darbha, S., et al. 2010, *MNRAS*, **406**, 2650
- Narayan, R., Piran, T., & Kumar, P. 2001, *ApJ*, **557**, 949
- O'Connor, B., Troja, E., & Gottlieb, A. 2022, GCN, 31376
- Paczynski, B. 1986, *ApJL*, **308**, L43
- Pe'er, A., Mészáros, P., & Rees, M. J. 2006, *ApJ*, **642**, 995
- Perley, D. A. 2021, GCN, 31323
- Perri, M., D'Elia, V., D'Ai, A., et al. 2021, GCN, 31327
- Pian, E., Antonelli, L. A., Piro, L., et al. 1998, GCN, 158
- Popham, R., Woosley, S. E., & Fryer, C. 1999, *ApJ*, **518**, 356
- Rastinejad, J. C., Fong, W., Kilpatrick, C. D., et al. 2021, *ApJ*, **916**, 89
- Rees, M. J., & Meszaros, P. 1994, *ApJL*, **430**, L93
- Rossi, A., Stratta, G., Maiorano, E., et al. 2020, *MNRAS*, **493**, 3379
- Rosswog, S., Davies, M. B., Thielemann, F.-K., et al. 2000, *A&A*, **526**, 575
- Rosswog, S., Korobkin, O., Arcones, A., et al. 2014, *MNRAS*, **439**, 744
- Sadler, E. M., Stathakis, R. A., Boyle, B. J., et al. 1998, *IAUC*, **6901**
- Sakamoto, T., Barthelmy, S. D., Barbier, L., et al. 2008, *ApJS*, **175**, 179
- Sari, R., & Piran, T. 1997, *ApJ*, **485**, 270
- Sari, R., Piran, T., & Narayan, R. 1998, *ApJL*, **497**, L17
- Savchenko, V., Ferrigno, C., Kuulkers, E., et al. 2017, *ApJL*, **848**, L15
- Stanek, K. Z., Matheson, T., Garnavich, P. M., et al. 2003, *ApJL*, **591**, L17
- Strausbaugh, R., & Cucchiara, A. 2021, GCN, 31321
- Tanvir, N. R., Levan, A. J., Fruchter, A. S., et al. 2013, *Natur*, **500**, 547
- Tanvir, N. R., Levan, A. J., González-Fernández, C., et al. 2017, *ApJL*, **848**, L27
- Thompson, C. 1994, *MNRAS*, **270**, 480
- Troja, E., Castro-Tirado, A. J., Becerra González, J., et al. 2019, *MNRAS*, **489**, 2104
- Troja, E., Piro, L., van Eerten, H., et al. 2017, *Natur*, **551**, 71
- Troja, E., Ryan, G., Piro, L., et al. 2018, *NatCo*, **9**, 4089
- Usov, V. V. 1992, *Natur*, **357**, 472
- Valenti, S., Sand, D. J., Yang, S., et al. 2017, *ApJL*, **848**, L24
- Wang, C.-J., Bai, J.-M., Fan, Y.-F., et al. 2019, *RAA*, **19**, 149
- Woosley, S. E. 1993, *ApJ*, **405**, 273
- Woosley, S. E., & Bloom, J. S. 2006, *ARA&A*, **44**, 507
- Xin, Y.-X., Bai, J.-M., Lun, B.-L., et al. 2020, *RAA*, **20**, 149
- Xu, D., de Ugarte Postigo, A., Leloudas, G., et al. 2013, *ApJ*, **776**, 98
- Yang, B., Jin, Z.-P., Li, X., et al. 2015, *NatCo*, **6**, 7323
- Yu, Y.-W., Liu, L.-D., & Dai, Z.-G. 2018, *ApJ*, **861**, 114
- Yu, Y.-W., Zhang, B., & Gao, H. 2013, *ApJL*, **776**, L40
- Yuan, Y., Lü, H.-J., Yuan, H.-Y., et al. 2021, *ApJ*, **912**, 14
- Zhang, B. 2013, *ApJL*, **763**, L22
- Zhang, B., Fan, Y. Z., Dyks, J., et al. 2006, *ApJ*, **642**, 354
- Zhang, B., & Mészáros, P. 2001, *ApJL*, **552**, L35
- Zhang, B., & Yan, H. 2011, *ApJ*, **726**, 90
- Zhang, B., Zhang, B.-B., Liang, E.-W., et al. 2007a, *ApJL*, **655**, L25
- Zhang, B., Zhang, B.-B., Virgili, F. J., et al. 2009, *ApJ*, **703**, 1696
- Zhang, B.-B., Liang, E.-W., & Zhang, B. 2007b, *ApJ*, **666**, 1002
- Zhang, B.-B., Liu, Z.-K., Peng, Z.-K., et al. 2021, *NatAs*, **5**, 911
- Zhang, B.-B., Zhang, B., Sun, H., et al. 2018, *NatCo*, **9**, 447